Improvement of superconducting properties of $FeSe_{0.5}Te_{0.5}$ single crystals by Mn substitution

A Günther[1], J Deisenhofer[1], Ch Kant[1], H-A Krug von Nidda[1], V Tsurkan[1,2] and A Loidl[1]

[1] Experimental Physics 5, Center for Electronic Correlations and Magnetism, Institute of Physics, University of Augsburg, D-86159 Augsburg, Germany
[2] Institute of Applied Physics, Academy of Sciences of Moldova, MD-2028, Chisinau, Republic of Moldova

Abstract

We report on structural, susceptibility, conductivity and heat-capacity studies of $FeSe_{0.5}Te_{0.5}$ single crystals with 2% substitution of Mn for Fe. Mn-doped samples show a higher onset temperature, a narrower width of the superconducting transition and a higher magnitude of the jump in the specific heat at T_c in comparison to undoped samples. The normal-state susceptibility exhibits a quasi-linear increase up to about 130 K. From the resistivity data in magnetic fields parallel to the c axis we derived an upper critical field H_{c2} of ∼420 kOe for doped samples compared to 370 kOe for pure samples. Using a single-band BCS model we can describe the electronic specific heat in the superconducting state with a gap $\Delta(T = 0) = 31$ K for the Mn-doped sample in comparison to 26 K for pure $FeSe_{0.5}Te_{0.5}$.

1. Introduction

Superconductivity in iron-based pnictides [1–3] and chalcogenides [4] is a hot topic in solid state and materials science. The iron chalcogenides forming the so-called '11' group are believed to require a much simpler description than pnictides with a more complicated structural arrangement. Slightly off-stoichiometric FeSe exhibits superconductivity at relatively low temperatures (∼8 K) [4]. However, the critical temperature T_c can be enhanced by external pressure up to 37 K [5, 6]. The superconducting properties of FeSe depend critically on the stoichiometry [7–9]. They can also be changed by different substitutions on the cation and anion sites. For example, substitution of Fe by transition metals such as Ti, V, Co, Ni and Cr destroys superconductivity [10, 11]. The substitution of Se by Te in FeSe increases T_c up to ∼14 K for 50% of replacement, e.g. $FeSe_{0.5}Te_{0.5}$ [12, 13], but T_c is suppressed with further increase of the Te concentration. Moreover, substitution of S for Te also induces superconductivity in FeTe and enhances the amount of the superconducting phase in FeSe [11, 14, 15]. In most cases mentioned above, bulk superconductivity is difficult to achieve. Indeed, in the best explored '11' system, $FeSe_{1-x}Te_x$, bulk superconductivity is reported only for $x \sim 0.5$, whereas for other concentrations the superconductivity is only filamentary. Even for the composition $x = 0.5$ the volume fraction of the bulk superconducting phase and the width of the superconducting transition vary rather significantly, depending on details of the preparation route [12, 16–20]. At present the origin of this behavior is far from being understood. The extreme sensitivity of the properties of the iron chalcogenides to minor deviations from the stoichiometry makes the elaboration of methods to stabilize their superconducting properties highly necessary.

Here we report on the properties of superconducting $FeSe_{0.5}Te_{0.5}$ single crystals with substitution of 2% Fe by Mn ions as studied by magnetic susceptibility, resistivity and specific heat. We find a clear increase of the onset temperature, a narrowing of the superconducting transition and an increased magnitude of the jump in the specific heat at T_c in the Mn-doped samples compared to those for the pure samples. Besides that, the doped samples exhibit a lower value of the susceptibility in the normal state, indicating a smaller content of magnetic impurities.

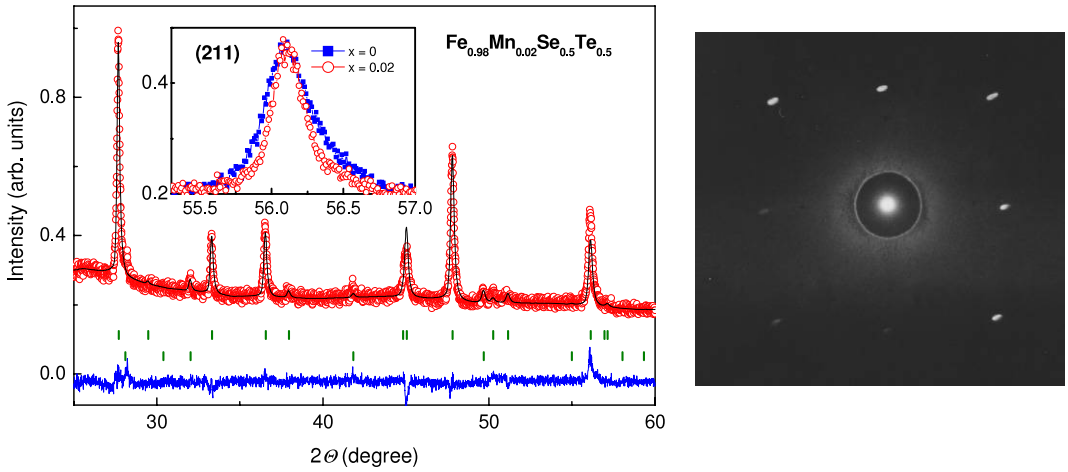

Figure 1. Left panel: experimental (red open circles) and refined (black solid line) x-ray diffraction patterns of $Fe_{0.98}Mn_{0.02}Se_{0.5}Te_{0.5}$. The bottom (blue) line represents the difference between the experimental and calculated intensities. The vertical (green) bars mark the Bragg positions of the main tetragonal phase (top) and of the impurity hexagonal phase (bottom). The inset shows the (211) reflection for the undoped (blue circles) and doped (red squares) samples. The right panel shows the Laue pattern for the Mn-doped sample.

2. Experimental details

Single crystals of pure and Mn-doped $FeSe_{0.5}Te_{0.5}$ were grown by the self-flux method in identical conditions. As the starting materials we used high-purity elements, 99.98% Fe (chips), 99.999% Se (chips), 99.999% Te and 99.99% Mn powder. To reduce the amount of oxide impurities, which have a significant influence on the superconducting properties [21], we additionally purified Se and Te by zone melting. Handling of the samples was performed in an argon box with residual oxygen and water content less than 1 ppm. Single crystals were grown in double quartz ampoules evacuated up to 10^{-3} mbar and sealed. Initial treatment was performed at 650 °C for 10 h followed by heating to 700 °C for 24 h. Further heating was performed up to 1100 °C with 72 h soaking at this temperature. After this the ampoule was cooled with a rate of 1 °C min^{-1} down to 400 °C for final annealing during 100 h followed by quenching in ice water. Plate-like samples with dimensions up to 5 mm × 3 mm × 0.5 mm were extracted from the solidified ingot. The Laue pattern for one of the grown single crystals is shown in the right panel of figure 1. The composition of the samples was checked by energy dispersive x-ray analysis (EDX). The EDX data are reported elsewhere [21]. The phase content of the samples was also analyzed by x-ray powder diffraction (Cu Kα radiation, $\lambda = 1.540\,560$ Å) on crushed single crystals using a STADI-P powder diffractometer (STOE & CIE) with a position-sensitive detector.

Magnetic measurements were performed in a temperature range of 2–400 K and in magnetic fields up to 50 kOe using a SQUID magnetometer (MPMS 5, Quantum Design). The heat capacity was measured by the relaxation method using a Quantum Design physical properties measurement system (PPMS) in a temperature range of 1.8–300 K and for magnetic fields up to 90 kOe. Resistivity studies were performed on rectangular samples by the four-point method using the resistivity measurement option of the PPMS with electrical contacts made of silver paint.

For comparison, we also show the experimental data for the best prepared earlier undoped sample (labeled as F216 step 1 in [21]).

3. Experimental results and discussion

The x-ray diffraction pattern for the Mn-doped sample together with the refined spectrum using the FULLPROF suite [22] is shown in the left panel of figure 1. The x-ray data were refined within tetragonal symmetry $P4/nmm$ [23] for the main $FeSe_{0.5}Te_{0.5}$ phase and within hexagonal symmetry $P63/mmc$ for the Fe_7Se_8 impurity phase. No other impurity phases were revealed by x-ray diffraction. The positions of Se and Te at the 2c sites were refined with different z coordinates. The occupation of Te and Se was refined, constraining the sum to unity in correspondence with the EDX analysis. A similar constraint was used for the occupation of Fe and Mn ions in the main phase. For the Fe ions two different sites (2a and 2c) [24] were allowed. The occupation factor for Mn was fixed at a nominal level of 2%. The results of the refinement for undoped and doped samples are given in table 1. Within the accuracy of the refinement we could not resolve the exact position of Mn. However, an enhanced value of the lattice constant c compared to the undoped samples suggests that the Mn ions occupy the 2c sites. If the larger Mn ions occupy the 2a positions an increase of the $a(b)$ parameter will be expected, while the experimental data exhibit an opposite trend. Therefore we concluded that the Mn ions preferably occupy the 2c sites. The refined occupation factors for Se and Te are close to their nominal concentrations. The refinement reveals a small amount of Fe ions (5%) present at the 2c sites in accord with observations in undoped samples [21]. The amount of the hexagonal impurity phase (4.7%) found in the doped samples was higher than in the undoped samples (1.4%). Rather astonishingly, the width of the reflections for the doped sample was narrower than for the undoped sample (see the inset in figure 1).

Table 1. Structural data obtained from the Rietveld refinement of $Fe_{1-x}Mn_xSe_{0.5}Te_{0.5}$.

Mn content, x	Occupation $Fe_1\|2a\|$	Occupation $Mn_2\|2c\|$	Occupation $Fe_2\|2c\|$	Occupation Se $\|2c\|$	Occupation Te $\|2c\|$	Lattice constant a, b (Å)	Lattice constant c (Å)	Tetragonal phase (%)	Hexagonal phase (%)
0	0.929(3)	—	0.071(3)	0.49(1)	0.51(1)	3.8025(3)	6.0300(9)	98.6	1.4
0.02	0.931(4)	0.02 fixed	0.049(4)	0.50(2)	0.50(2)	3.8013(3)	6.0600(9)	95.3	4.7

Figure 2(a) shows the temperature dependence of the zero-field-cooled (ZFC) and field-cooled (FC) susceptibility for the doped sample measured in a field of 10 Oe applied along the c axis. The ZFC susceptibility shows a sharp transition into the superconducting state with an onset temperature T_c^{on} of 14.4 K which is higher than for the undoped sample (13.9 K), as can also be deduced from the FC susceptibility shown on an enlarged scale in the inset of this figure. The transition width, determined as the difference between the onset temperature and the intercept of the steepest part of the ZFC susceptibility extrapolated to the temperature axis, is markedly smaller for the Mn-doped sample (1.0 K) than for the undoped sample (1.5 K). The value of the FC susceptibility (Meissner effect) is rather low, indicating strong flux-pinning. The value of the susceptibility just above the transition for the Mn-doped sample is about eight times lower than for the undoped sample, suggesting a lower content of magnetic impurities. The diamagnetic ZFC susceptibility (shielding effect) is more than two orders of magnitude higher than the FC susceptibility. The calculated value of $4\pi\chi$ from the ZFC data at 2 K is far above unity, suggesting the influence of demagnetizing effects. Measurements of needle-like samples cut from the original samples with a negligible demagnetizing factor in magnetic fields applied along the long side yielded a value of $4\pi\chi$ close to unity, indicating the bulk character of the susceptibility.

Figure 2(b) shows the temperature dependences of the magnetic susceptibility measured on cooling in a field of 10 kOe along the c axis in an extended temperature range 2 K $< T <$ 400 K. The susceptibility of the doped sample manifests a non-monotonic temperature dependence with a broad maximum at around 180 K, similar to that observed in the undoped sample. However, the overall variations of the susceptibility for the doped sample are much more pronounced in the normal and in the superconducting states. Beside this, the doped sample exhibits a lower susceptibility in the normal state. Previous studies of $FeSe_{0.5}Te_{0.5}$ single crystals prepared under different conditions [21] have shown that iron oxide (magnetite, Fe_3O_4) is the main magnetic impurity present in samples handled in air or prepared from non-purified elements. The susceptibility of the samples containing oxide impurities is significantly higher than that of the oxygen-free samples. The undoped sample has minimal content of the magnetic oxide impurity [21]. Therefore, an even smaller value of the magnetic susceptibility of the Mn-doped sample may indicate a further reduction of magnetic impurities and reveal the intrinsic magnetic susceptibility of the $FeSe_{0.5}Te_{0.5}$ system. We must also note that the doped sample contains a nearly three times higher amount of the impurity phase of Fe_7Se_8 than the undoped sample (table 1). This suggests that Fe_7Se_8 has an insignificant effect on the magnetic and superconducting properties of the doped samples

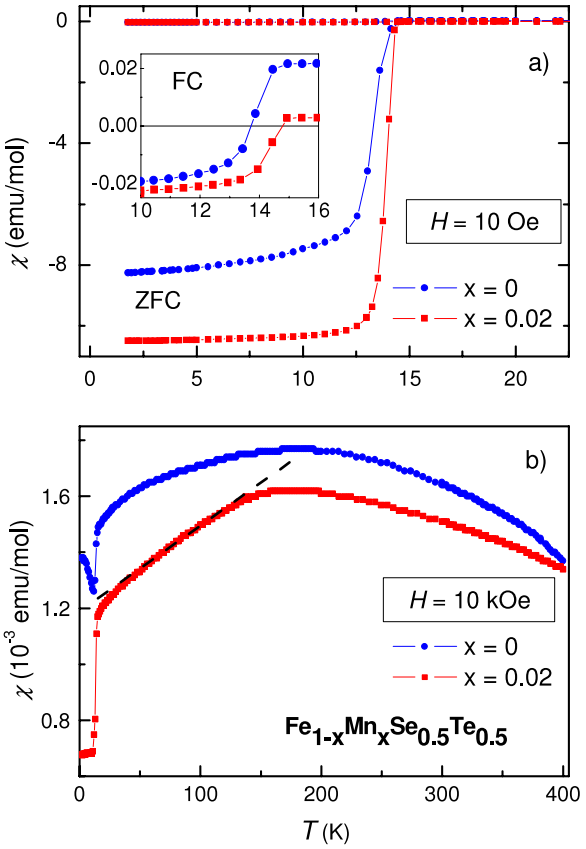

Figure 2. (a) Temperature dependences of ZFC and FC susceptibilities for undoped ($x = 0$) and doped ($x = 0.02$) single-crystalline samples measured in a field of 10 Oe applied along the c axis in the low-temperature range. The inset shows the FC susceptibility on an enlarged scale. (b) Temperature dependences of the susceptibility for both samples measured in a field of 10 kOe applied along the c axis in the range 2 K $<$ T $<$ 400 K. The dashed line shows a linear character of the susceptibility above T_c up to 130 K for the doped sample.

and confirms the earlier conclusion of [21] which excluded Fe_7Se_8 from factors suppressing bulk superconductivity in $FeSe_{0.5}Te_{0.5}$. It must also be mentioned that the larger drop of the susceptibility at T_c and the absence of any upward behavior towards the lowest temperatures, as observed in the doped sample, suggests a more robust superconducting state resulting from Mn substitution.

Above T_c the susceptibility of the Mn-doped sample exhibits a quasi-linear increase up to about 130 K, similar to linearly increasing normal-state susceptibilities in the '1111' and '122' compounds [25]. We are not aware of any other reported linearly increasing susceptibility in $FeSe_{0.5}Te_{0.5}$ single crystals to date and believe that our data are very close to the intrinsic susceptibility in agreement with Knight

Table 2. Parameters of superconducting and normal state for $Fe_{1-x}Mn_xSe_{0.5}Te_{0.5}$ calculated from the magnetic, resistivity and specific heat data.

Mn content, x	T_c^{onset} (K) from χ_{ZFC}	$T_c^{0.1R_n}$ (K) from ρ	j_c (2 K) (kA cm^{-2})	H_{c2} (0) (kOe) [$H \parallel c$]	γ_r (mJ mol^{-1} K^{-2})	β (mJ mol^{-1} K^{-4})	γ_n (mJ mol^{-1} K^{-2})	Δ_0 (K)	$2\Delta_0/T_c$
0	13.9	13.6	86	370[a] 980[b]	0.96	0.94	25	26	3.57
0.02	14.4	14.4	85	420[a] 1230[b]	1.88	0.74	30	31	4.47

[a] Estimated from the resistivity. [b] Estimated from the specific heat.

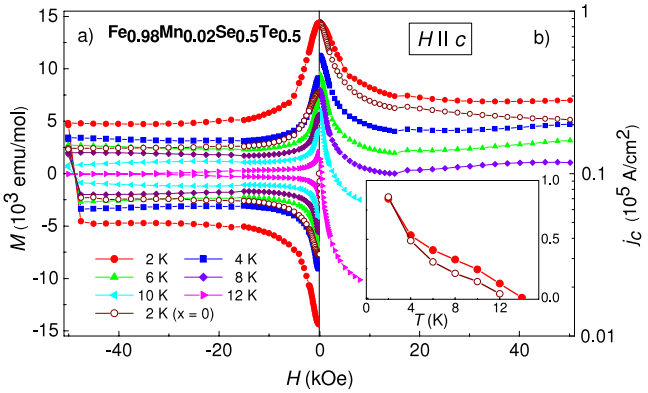

Figure 3. (a) Hysteresis loops of the Mn-doped sample (full symbols) at different temperatures and of the undoped sample (open circles) for 2 K measured with the field applied along the c axis. (b) Critical current density j_c versus magnetic field at different temperatures for the Mn-doped sample (full symbols) and for the undoped sample at 2 K (open circles). The inset shows the temperature dependence of the critical currents at zero field for undoped (open circles) and doped (closed circles) samples. Sample dimensions: undoped—1.65 × 3.2 × 0.5 mm^3; doped—3.4 × 4.75 × 0.5 mm^3.

shift data obtained from NMR in a superconducting single crystal of $Fe_{1.04}Se_{0.33}Te_{0.67}$ (with $T_c = 14$ K), which reveals a linear increase up to 100 K [26]. Several scenarios including strong antiferromagnetic spin fluctuations or electronic band-structure effects have been discussed as the possible origin of this linear increase (see [27] and references therein). Whatever the underlying physical mechanism is, we think that the observed quasi-linear susceptibility in our '11'-type sample shows a common feature for all three classes of Fe-based superconductors. The reason for the decrease at higher temperatures is not clear, but we would like to stress the similarity of the overall susceptibility with two-dimensional antiferromagnetically coupled spin systems [28].

Figure 3 presents the left half (a) of a symmetric magnetization hysteresis loop for the Mn-doped sample measured at different temperatures. In the same figure the 2 K data for the undoped sample are shown by open circles. The field dependence of the critical current density j_c estimated using the Bean model for hard superconductors [29, 30] is shown in the right half (b) of figure 3 for different temperatures. At 2 K the critical current density j_c of 8.5 × 10^4 A cm^{-2} at zero field was determined for the Mn-doped sample. For the undoped samples we obtained a similar value of j_c at zero field. At the same time, at higher fields the doped samples exhibit larger critical currents (by ∼20%) than the undoped ones, indicating the presence of additional pinning centers. Above 20 kOe up to the largest measured fields the critical current is only slightly field-dependent, suggesting a high current-carrying ability. The inset of figure 3(b) compares the temperature dependences of the critical current j_c at $H = 0$ for doped and undoped samples. For the undoped sample the value of the critical currents $j(0) = 1.7 \times 10^5$ A cm^{-2} (for $T = 0$ K) was estimated from the fit to the experimental data using a power-law dependence $j(T) = j(0)[1 - (T/T_c)^p]^n$, with $p = 0.5$, $n = 1.5$ and $T_c = 13.8$ K. For the doped sample in the measured temperature range such an extrapolation was not possible, but from the experimental data of this sample one can expect a similar high value of the critical current density for $T = 0$ K. We additionally notice that j_c in the doped sample decreases with temperature not as fast as in the undoped sample, indicating a higher current-carrying ability on approaching T_c. The critical current density calculated from the hysteresis loops at 2 K together with the critical temperature T_c determined from the magnetic data are given in table 2.

Figure 4(a) presents the temperature dependences of the resistivity for the doped sample around the superconducting transition compared with the data for the undoped sample. Similarly to the susceptibility data, the resistive transition for the doped sample is significantly steeper and is shifted by 0.5 K to higher temperatures. The temperature of the superconducting transition determined using the criterion of a 90% drop of the normal-state resistivity R_n for the doped sample is 14.4 K and fits perfectly the onset temperature T_c^{on} determined from the low-field susceptibility. This confirms the high purity of the doped samples. The resistivity of the doped sample reveals a metal-like increase above T_c up to 200 K, similar to that observed in the undoped samples [21]. Such a metal-like behavior was established earlier for $FeSe_{1-x}Te_x$ with a low amount of excess iron [31]. In the normal state the Mn-doped sample exhibits a higher resistivity compared to the undoped sample, which suggests an increased scattering of charge carriers on impurity centers which can be associated with the Mn ions.

In figure 4(b) the temperature dependences of the resistivity taken at different magnetic fields in the transition range are presented for the Mn-doped sample. The magnetic field was applied parallel to the c axis. The measurements were performed on warming after cooling in zero field. The resistivity curves exhibit a gradual shift to lower temperatures with increasing magnetic field, similar to reports on undoped samples [21]. The temperature dependences of the upper critical field $H_{c2}(T)$ determined using the criterion of a 90% drop of the normal-state resistivity R_n is presented in the inset of figure 4(b). The values of the upper critical field $H_{c2}(0)$

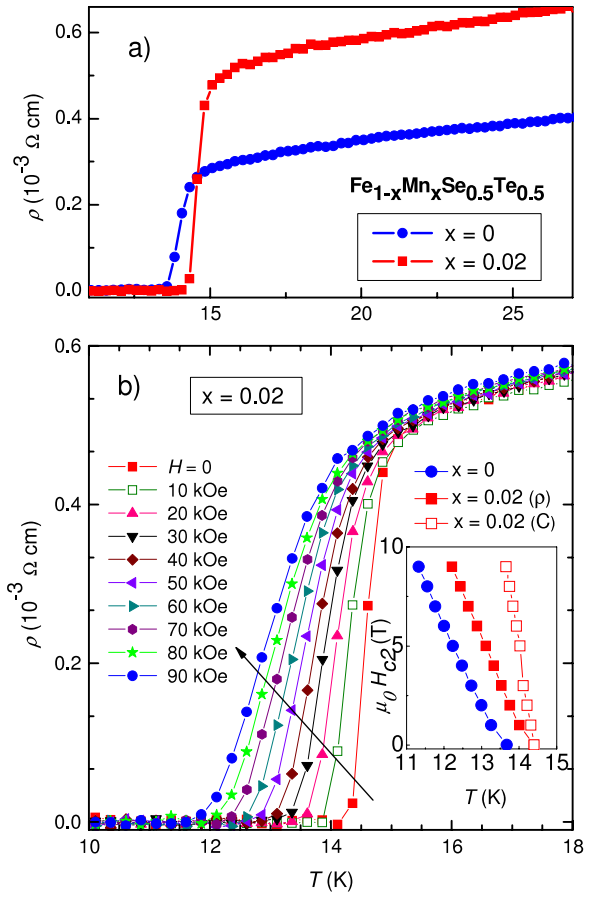

Figure 4. (a) Temperature dependences of the in-plane resistivity for undoped and Mn-doped samples measured in zero field. (b) Temperature dependences of the in-plane resistivity for the Mn-doped sample measured at various magnetic fields applied parallel to the c axis. The inset shows the temperature dependences of the upper critical field H_{c2} for undoped and Mn-doped samples (closed symbols) calculated from the resistivity data. Open squares represent $H_{c2}(T)$ for the doped sample calculated from the specific heat and shifted by 0.32 K on the temperature axis to fit the onset of the resistivity data.

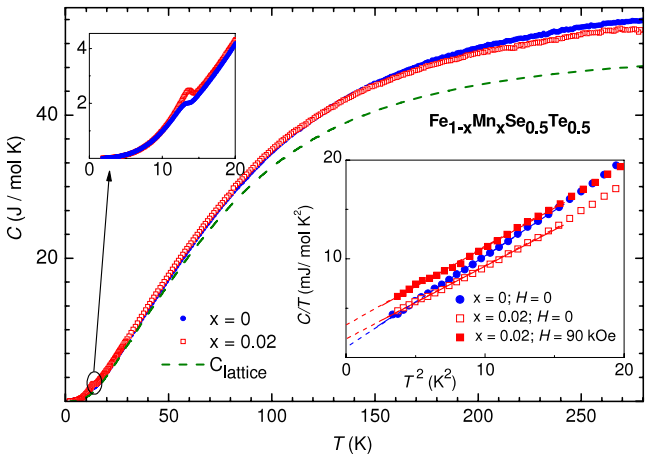

Figure 5. Temperature dependences of the specific heat for the undoped and Mn-doped samples. The dashed line represents the lattice specific heat calculated using the combined Debye–Einstein model as described in the text. The upper inset shows the specific heat in the transition region on an enlarged temperature scale. The lower inset shows the temperature dependences of the specific heat in the representation C/T versus T^2 for the temperature range 1.8–4.5 K for $H = 0$ and 90 kOe.

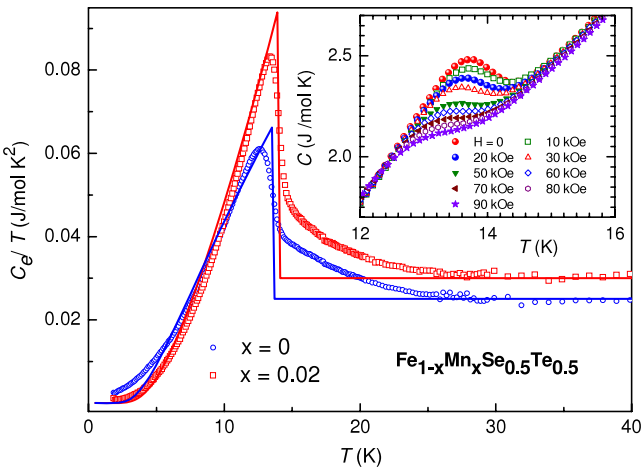

Figure 6. Temperature dependences of the electronic specific heat as C_e/T versus T for Mn-doped (open squares) and undoped (open circles) samples. The solid lines represent the fits describing the superconducting specific heat within the BCS model. The inset shows the temperature dependences of the specific heat in different applied magnetic fields for the Mn-doped sample.

for $T = 0$ K were estimated using the expression $H_{c2}(0) = -0.69T_c(dH_{c2}(T)|dT)|_{T_c}$ defined by the Werthamer–Helfand–Hohenberg (WHH) model [32]. The calculated results are presented in table 2. The estimated value of $H_{c2}(0) \sim 420$ kOe is higher for the Mn-doped samples than for the undoped sample (370 kOe) and can probably be attributed to enhanced impurity scattering from the Mn ions.

Figure 5 shows the temperature dependence of the specific heat C for the Mn-doped sample. Above the superconducting transition up to a temperature of 150 K, $C(T)$ is close to that of the undoped sample shown in the same figure. The upper inset in figure 5 illustrates the specific heat in the low-temperature range. A pronounced anomaly at T_c is shown with a much larger specific heat jump for the Mn-doped sample when compared to the undoped one. Magnetic field (applied parallel to the c axis) suppresses the anomaly in the specific heat at T_c displacing it to lower temperatures (see the inset in figure 6). From the shift of the minimum of the temperature derivative of the electronic specific heat in the transition region the upper critical field H_{c2} was determined. It is shown by open squares in the inset of figure 4. We found a significant difference between the $H_{c2}(T)$ determined from the resistivity and from the specific heat, the latter being much closer to $H_{c2}(T)$ derived from the resistivity curves for the field parallel to the *ab* plane [21]. The estimations using the WHH formula [32] gave a value of $H_{c2}(0) \sim 1230$ kOe which is, by a factor of 3, larger than that obtained from the resistivity data. The reason for this difference is unclear at present and is beyond the scope of this paper. However, it must be noted that a similar large difference in $H_{c2}(0)$ determined from the resistivity and specific heat was reported recently for superconducting $Ba(K)Fe_2As_2$ [33] and

$FeSe_{1-x}Te_x$ (with $x = 0.52$) [34] and was tentatively ascribed to anisotropic vortex dynamics.

In the lower inset in figure 5 the temperature dependences of the specific heat for the doped sample are shown as C/T versus T^2 at temperatures below 4.5 K, measured in zero field and in a field of 90 kOe. By a fit to the experimental data in the range below 4.5 K using the expression $C/T = \gamma + \beta T^2$ we determined the values of the residual Sommerfeld coefficient γ_r, related to the electronic contribution, and the prefactor β characterizing the lattice contribution to the specific heat. The respective data are given in table 2. For the Mn-doped sample a value of $\gamma_r \sim 1.9$ mJ mol^{-1} K^{-2} was obtained which is, by a factor of two, larger than the one for the undoped sample ($\sim$1 mJ mol^{-1} K^{-2} [21]). These extremely low values of γ_r are, to the best of our knowledge, the smallest reported so far for $FeSe_{1-x}Te_x$ and thus confirm the high quality of our samples.

The dependences of the electronic specific heat in the representation C_e/T versus T are shown in figure 6 for a temperature range around the superconducting transition. The electronic specific heat was calculated by subtraction of the lattice contribution from the total specific heat. The lattice contribution was estimated within a combined Debye–Einstein model used in [21] for the undoped $FeSe_{0.5}Te_{0.5}$ samples with high volume fraction of the superconducting phase and for those with fully suppressed superconductivity. Twelve normal modes of vibrations of the tetragonal unit cell of FeSe(Te) were simulated by two Debye terms C_D and one Einstein term C_E with equal distribution of the spectral weight between the Debye and Einstein terms in agreement with the experimental study of the phonon density of states in FeSe superconductors by nuclear inelastic scattering [35] and neutron scattering [36]. The characteristic Debye and Einstein temperatures, Θ_D and Θ_E, were the input parameters for a fit to the experimental temperature dependence of the total specific heat above T_c by the expression

$$C = C_{D1}(\Theta_{D1}) + C_{D2}(\Theta_{D2}) + C_E(\Theta_E) + \gamma_n T,$$

where γ_n is the Sommerfeld coefficient in the normal state. The fitting parameters were varied until the minimal deviations from a constant value of γ_n in a maximal temperature range (above T_c up to 200 K) were achieved. The temperature dependence of the simulated lattice specific heat with the values of $\Theta_{D1} = 127$ K, $\Theta_{D2} = 235$ K and $\Theta_E = 315$ K is shown by the dashed line in figure 5. With this lattice contribution we obtained for the Sommerfeld coefficient in the normal state a value of $\gamma_n = 30$ mJ mol^{-1} K^{-2}, which is slightly higher than that of 25 mJ mol^{-1} K^{-2} for the undoped sample [21]. It is important to note that these values of γ_n are much lower than those reported previously for $FeSe_{1-x}Te_x$ by other authors [16, 31, 37]. The reason for this discrepancy is related to different estimates of the lattice contribution. In particular, high values of γ_n of the order of 100 mJ mol^{-1} K^{-2} were reported in several papers on FeSe(Te) [4, 26] which used an odd-power polynomial fit to the experimental data taken just above T_c to separate the electronic and lattice specific heat. Utilizing a similar fitting procedure for the temperature range 15–21 K we indeed obtained for the normal electronic coefficient γ_n a rather high value of $\sim$100 mJ mol^{-1} K^{-2} for the Mn-doped sample and $\sim$90 mJ mol^{-1} K^{-2} for the undoped one [21]. At the same time, the prefactor β was determined as 0.28 mJ mol^{-1} K^{-4} for the Mn-doped sample and 0.3 mJ mol^{-1} K^{-4} for the undoped sample, corresponding to Debye temperatures Θ_D of 190 K and 235 K for these samples, respectively. However, this simple Debye approximation is known to work well only for temperatures below $\Theta_D/50$ [38], e.g. below $\sim$5 K, which is much lower than the temperature range of fitting. Therefore the values of γ_n obtained by such extrapolation are strongly overestimated. In [21] it was shown that for the $FeSe_{0.5}Te_{0.5}$ with suppressed bulk superconductivity the lattice specific heat calculated by the subtraction of the electronic specific heat $\gamma_n T$ (with $\gamma_n = 23$ mJ mol^{-1} K^{-2}) from the total (measured) specific heat perfectly coincides with the lattice contribution simulated within the above-mentioned Debye–Einstein model. We additionally note that no scaling of the lattice specific heat for the samples with the pronounced bulk superconductivity and for those with suppressed bulk superconductivity was necessary in this case. These arguments strongly support the validity of the approximation used to estimate the lattice specific heat.

As shown in figure 6 the electronic specific heat for the Mn-doped sample manifests a sharp anomaly at around T_c with a much higher jump in the specific heat at the superconducting transition than for the undoped sample. At the same time, above T_c a tail in the electronic specific heat is shown, extending to a temperature of 30 K. A similar tail in the electronic specific heat above T_c was observed for the undoped $FeSe_{0.5}Te_{0.5}$ both for the samples with full bulk superconductivity and with suppressed bulk superconductivity [21]. Importantly, for the samples with suppressed bulk superconductivity this anomaly evolves at temperatures below 15 K as a broad peak with a Schottky-like appearance. indicating an electronic origin. Moreover, this anomaly is independent of the magnetic field (up to 90 kOe), suggesting a probable relation to the orbital degrees of freedom. In [21] this broad anomaly was attributed to a splitting of a ground state of Fe^{2+} ions either by crystal field or spin–orbital coupling. It was described within a model of a two-level system with the value of the ground-state splitting of $\Delta = 24$ cm^{-1} with a concentration of magnetic ions corresponding to 7 mol%. They were associated with the minority Fe^{2+} ions at 2c positions in the chalcogen plane shown by x-ray refinement. These ions are expected to carry a local magnetic moment [14, 24, 31].

It must be noted that a remarkably sharp behavior of the specific heat just below T_c observed both in the Mn-doped and in the undoped samples with pronounced bulk superconductivity (figure 6) along with their extremely low values of the residual Sommerfeld coefficient γ_r (inset of figure 5) and the strong dependence of the specific heat on the magnetic field below T_c (inset of figure 6) indicate that the Schottky-like contribution is fully suppressed in the superconducting state. At the same time, the presence of the Schottky-like anomaly at temperatures below 14 K in samples with suppressed bulk superconductivity might indicate the

existence of competing interactions. When superconductivity sets in, the Schottky-like contribution is quenched, while in the case of suppression of the bulk superconductivity it remains observable. The reason for this quenching as well as the suppression of the bulk superconductivity is unclear at present and needs additional studies. But in any case, these facts allow us to neglect the Schottky-like contribution below T_c in the superconducting samples when analyzing the electronic specific heat.

The other possibility of appearance of a tail in the specific heat above T_c may be related to magnetic fluctuations, which was one scenario suggested to explain the quasi-linear increase of the normal-state spin susceptibility as discussed above. Moreover, NMR studies also show the existence of spin fluctuations above T_c [26]. Note that the Mn-doped sample contains the minimal amount of magnetic impurities. In samples with higher magnetic impurity content this behavior is masked, for example like in those containing Fe_3O_4 which exhibit a monotonic increase of the magnetic susceptibility on decreasing temperature [21]. To arrive at final conclusions more comprehensive studies are certainly necessary.

The temperature behavior of the electronic specific heat in the superconducting state was analyzed within the BCS-derived α model [39, 40] with a temperature-dependent superconducting gap Δ similar to the analysis of the specific heat in related (Ba:K)Fe_2As_2 pnictides [41, 42]. The fitted results for the electronic specific heat are shown in figure 6 by solid lines.

From the ratio of the residual Sommerfeld coefficient γ_r to that of the normal state γ_n we obtained a value $\sim$0.06 for the Mn-doped sample corresponding to a volume fraction of the superconducting phase of 94%. This is slightly lower than $\sim$96% obtained for the undoped sample. Despite the lower volume fraction of the superconducting phase, the doped sample manifests a significantly higher magnitude of the jump in the specific heat at the superconducting transition. Certainly this fact has to be attributed to the substitution effect. It may result, for example, from the increased density of states at the Fermi level, as can be concluded from the higher value of the normal Sommerfeld coefficient (table 2). Note that the amount of the non-superconducting phase in both samples roughly correlates with the amount of Fe_7Se_8. However, this impurity phase, as was already noted above, does not suppress the superconductivity of the $FeSe_{0.5}Te_{0.5}$. Therefore in samples prepared without Fe_7Se_8 impurity one would expect an even lower residual Sommerfeld coefficient.

Although the Fe-based superconductors are evidently multi-band systems with possibly multiple gaps, it was found that a single-band BCS model can describe the superconducting specific heat reasonable well [42–44]. The deviations below 5 K are probably related to effects of residual impurities. The value of the superconducting gap at 0 K is determined as $\Delta_0 = 31$ K (2.7 meV) for an Mn-doped sample and is higher than $\Delta_0 = 26$ K obtained for the undoped sample [21]. This value is in fair agreement with the value of 2.3 meV obtained by Kato *et al* [45] from the tunneling spectroscopy and with the low-energy gap of 2.5 meV observed by Homes *et al* [46] in the optical conductivity of $FeSe_{0.45}Te_{0.55}$, as well as with 2.6 meV obtained by Biswas *et al* [47] from μSR, and by Bendele *et al* [48] from magnetic penetration studies of $FeSe_{0.5}Te_{0.5}$. It seems that in our case the specific heat is dominated by the smallest gap, similar to K-doped $BaFe_2As_2$, and the BCS model allows us to estimate the smallest gap with good accuracy [41, 42]. This rather good correlation between the value of the superconducting gap derived from the specific heat with that determined by other independent techniques additionally justifies our approach for the analysis of the superconducting and lattice contributions to the specific heat. Finally, we want to mention that the obtained ratio $2\Delta_0/T_c = 4.47$ is larger than the universal weak-coupling single-band BCS value of 3.53. The BCS model, however, should only be regarded as a parameterization of the underlying multi-band contributions to the specific heat and hence deviations from the universal one-band value cannot easily be attributed to the coupling strength [43].

4. Concluding remarks

In conclusion, our studies of the properties of $FeSe_{0.5}Te_{0.5}$ single crystals doped with 2% Mn reveal a clear change of their structural, magnetic and superconducting parameters. The doped samples show narrower x-ray diffraction lines than undoped samples, suggesting a higher homogeneity. The lower value of the susceptibility in the normal state for the doped samples indicates a smaller content of the magnetic impurities compared to the undoped samples. The observed quasi-linear increase of the normal-state susceptibility is consistent with observations in the '122' and '1111' systems and with the NMR Knight shift reported for comparable '11' single crystals. The Mn doping obviously has a positive effect on the superconducting properties. Although the observed increase of the onset temperature T_c^{on} (by $\sim$0.5 K) for the doped sample is not large, we found a pronounced narrowing of the superconducting transition and an enhanced magnitude of the jump in the specific heat at T_c compared to the undoped samples. For the doped samples the critical current density at high fields and the upper critical field are also notably enhanced compared to those for the undoped samples.

We note that very recently an enhanced T_c^{on} of 14.9 K in the resistive transition on polycrystalline $FeSe_{0.5}Te_{0.5}$ doped with 5% Mn was reported by Zhang *et al* [49], supporting our single-crystalline data. However, there is a notable difference between their susceptibility data and our results. Beside this, their data for the resistivity in the normal state show an opposite trend compared to our data.

Considering the enhancement of the superconducting parameters in $FeSe_{0.5}Te_{0.5}$ by Mn doping, it should be noted that this effect is in contrast to '122' Fe-based superconducting systems, where Mn doping leads to pair-breaking resulting in a considerable reduction of the superconducting transition temperature even at such a low level of substitution as 2% [50]. The mechanisms of pair-breaking in Fe-based superconductors are far from being established. Our present experiments allow us to exclude several reasons for the observed changes of properties of $FeSe_{0.5}Te_{0.5}$ by Mn doping. They confirm the previous conclusions [21] about the insignificant role of

the hexagonal impurity phase of Fe_7Se_8 in suppressing the superconductivity in $FeSe_{0.5}Te_{0.5}$. Discussing the role of the magnetic Fe ions at the 2c site, which are assumed to suppress the superconductivity in the '11' system [14, 20, 24, 31], we would like to note that studies of the undoped $FeSe_{0.5}Te_{0.5}$ samples with a high volume fraction of the superconducting phase and of those with strongly suppressed superconductivity put a question mark on the validity of this assumption, at least for the samples with low amounts of excess Fe ions. To our opinion, the most plausible explanation of the observed doping effect is related to a reduction of the residual ferrimagnetic iron oxide impurities due to formation of antiferromagnetic manganese oxides. As was already established in [21], samples containing magnetic oxide impurities exhibit an enhanced susceptibility in the normal state, a reduced onset temperature and reduced magnitude of the jump of the specific heat at T_c compared to samples with a lower content of oxide impurities. The amount of the residual iron oxide impurities in the best undoped samples discussed in [21] is below 0.1 mol% as estimated from the change of their susceptibility compared to the impure samples. A further reduction of the susceptibility, an increase of the transition temperature T_c and strong enhancement of the jump in the specific heat at T_c observed in the Mn-doped sample suggest that the significant changes of the material properties are caused by a rather subtle variation of tuning parameters, most probably due to residual iron oxide impurities. Of course, for a larger concentration, the substitution can have an opposite effect and Mn can behave in a similar way as the other transition metals that suppress the superconductivity in FeSe [10, 11] and $FeSe_{0.5}Te_{0.5}$ [49]. It is clear that, to clarify the role of doping and the origin of the observed changes of the magnetic and superconducting parameters, complete doping series are necessary. These experiments are currently in progress. However, already the present results demonstrate a substantial effect of Mn doping on the properties of $FeSe_{0.5}Te_{0.5}$ and we hope that they will stimulate further experimental and theoretical studies of the interesting '11' superconductors.

Acknowledgments

The authors thank Dana Vieweg and Klaus Wiedenmann for experimental support. This research has been supported by the DFG via SPP 1458 and via the Transregional Collaborative Research Center TRR 80 (Augsburg Munich).

References

[1] Kamihara Y, Watanabe T, Hirano M and Hosono H 2008 *J. Am. Chem. Soc.* **130** 3296
[2] Rotter M, Tegel M and Johrendt D 2008 *Phys. Rev. Lett.* **101** 107006
[3] Tapp J H, Tang Z, Lv B, Sasmal K, Lorenz B, Chu C W and Guloy A M 2009 *Phys. Rev.* B **78** 060505
[4] Hsu F C *et al* 2008 *Proc. Natl Acad. Sci. USA* **105** 14262
[5] Medvedev S *et al* 2009 *Nat. Mater.* **8** 630
[6] Margadonna S, Takabayashi Y, Ohishi Y, Mizuguchi Y, Takano Y, Kagayama T, Nakagawa T, Takata M and Prassides K 2009 *Phys. Rev.* B **80** 064506
[7] McQueen T M *et al* 2009 *Phys. Rev.* B **79** 014522
[8] Pomjakushina E, Conder K, Pomjakushin V, Bendele M and Khasanov R 2009 *Phys. Rev.* B **80** 024571
[9] de Souza M, Haghighirad A A, Tutsch U, Assmus W and Lang M 2010 *Eur. Phys. J.* B **77** 101
[10] Wu M K *et al* 2009 *Physica* C **469** 340
[11] Mizuguchi Y, Tomioka F, Tsuda S, Yamaguchi T and Takano Y 2009 *J. Phys. Soc. Japan* **78** 074712
[12] Fang M H, Pham H M, Qian B, Liu T J, Vehstedt E K, Liu Y, Spinu L and Mao Z Q 2008 *Phys. Rev.* B **78** 224503
[13] Yeh K W *et al* 2008 *Europhys. Lett.* **84** 37002
[14] Hu R, Bozin E S, Warren J B and Petrovic C 2009 *Phys. Rev.* B **80** 214514
[15] Mizuguchi Y, Tomioka F, Tsuda S, Yamaguchi T and Takano Y 2009 *Appl. Phys. Lett.* **94** 012503
[16] Sales B C, Sefat A S, McGuire M A, Jin R Y, Mandrus D and Mozharivskyj Y 2009 *Phys. Rev.* B **79** 094521
[17] Taen T, Tsuchiya Y, Nakajima Y and Tamegai T 2009 *Phys. Rev.* B **80** 092502
[18] Noji T, Suzuki T, Abe T, Adachi T, Kato M and Koike Y 2010 *J. Phys. Soc. Japan* **79** 084711
[19] Tegel M, Loehnert C and Johrendt D 2010 *Solid State Commun.* **150** 383
[20] Viennois R, Giannini E, van der Marel D and Černy R 2010 *J. Solid State Chem.* **183** 769
[21] Tsurkan V, Deisenhofer J, Günther A, Kant Ch, Krug von Nidda H A, Schrettle F and Loidl A 2011 doi:10.1140/epjb/e2010-10473-5
[22] Rodriguez-Carvajal J 1993 *Physica* B **192** 55
[23] Hahn T (ed) 1996 *International Tables for Crystallography* (Dordrecht: Kluwer Academic) v. A.
[24] Li S *et al* 2009 *Phys. Rev.* B **79** 054503
[25] Klingeler R *et al* 2010 *Phys. Rev.* B **81** 024506
[26] Michioka C, Ohta H, Matsui M, Yang J, Yoshimura K and Fang M 2010 *Phys. Rev.* B **82** 064506
[27] Johnston D C 2010 *Adv. Phys.* **59** 803
[28] de Jongh L J (ed) 1989 *Magnetic Properties of Layered Transition Metal Compounds* (Dordrecht: Kluwer Academic)
[29] Bean C P 1962 *Phys. Rev. Lett.* **8** 250
[30] Bean C P 1964 *Rev. Mod. Phys.* **36** 90
[31] Liu T J *et al* 2009 *Phys. Rev.* B **79** 174509
[32] Werthamer N R, Helfand E and Hohenberg P C 1966 *Phys. Rev.* **147** 295
[33] Popovich P, Boris A V, Dolgov O V, Golubov A A, Sun D L, Lin C T, Kremer R K and Keimer B 2010 *Phys. Rev. Lett.* **105** 027003
[34] Braithwaite D, Lapertot G, Knafo W and Sheikin I 2010 *J. Phys. Soc. Japan* **79** 053703
[35] Ksenofontov V, Wortmann G, Chumakov A I, Gasi T, Medvedev S, McQueen T M, Cava R J and Felser C 2010 *Phys. Rev.* B **81** 184510
[36] Phelan D, Millican J N, Thomas E L, Leao J B, Qiu Y and Paul R 2009 *Phys. Rev.* B **79** 014519
[37] Zeng B, Mu G, Luo H Q, Xiang T, Yang H, Shan L, Ren C, Mazin I, Dai P C and Wen H H 2010 arXiv:1004.2236 unpublished
[38] Kittel C 1971 *Introduction to Solid State Physics* (New York: Wiley)
[39] Bouquet F, Wang Y, Fisher R A, Hinks D G, Jorgensen J D, Junod A and Phillips N E 2001 *Europhys. Lett.* **56** 856
[40] Padamsee H, Neighbor J E and Shiffman C A 1973 *J. Low Temp. Phys.* **12** 387
[41] Rotter M, Tegel M, Schellenberg I, Schappacher F M, Pöttgen R, Deisenhofer J, Günther A, Schrettle F, Loidl D and Johrendt D 2009 *New J. Phys.* **11** 025014

[42] Kant Ch, Deisenhofer J, Günther A, Schrettle F, Loidl A, Rotter M and Johrendt D 2010 *Phys. Rev.* B **81** 014529
[43] Benfatto L, Cappelluti E and Castellani C 2009 *Phys. Rev.* B **80** 214522
[44] Serafin A, Coldea A I, Ganin A Y, Rosseinsky M J, Prassides K, Vignolles D and Carrington A 2010 *Phys. Rev.* B **82** 104514
[45] Kato T, Mizuguchi Y, Nakamura H, Machida T, Sakata H and Takano Y 2009 *Phys. Rev.* B **80** 180507(R)
[46] Homes C C, Akrap A, Wen J S, Xu Z J, Lin Z W, Li Q and Gu G D 2010 *Phys. Rev.* B **81** 180508
[47] Biswas P K, Balakrishnan G, Paul D M, Tomy C V, Lees M R and Hillier A D 2010 *Phys. Rev.* B **81** 092510
[48] Bendele M *et al* 2010 *Phys. Rev.* B **81** 224520
[49] Zhang A M, Xia T L, Kong L R, Xiao J H and Zhang Q M 2010 *J. Phys.: Condens. Matter* **22** 245701
[50] Cheng P, Shen B, Hu J and Wen H H 2010 *Phys. Rev.* B **81** 174529